Frizzled regulates localization of cell-fate determinants and mitotic spindle rotation during asymmetric cell division

Yohanns Bellaïche*, Michel Gho*, Julia A. Kaltschmidt†, Andrea H. Brand† and François Schweisguth*‡

**Ecole Normale Supérieure, UMR 8544, 46, rue d'Ulm, 75230 Paris Cedex 05 France*

†Wellcome/CRC Institute and Department of Genetics, University of Cambridge, Tennis Court Road, Cambridge, CB2 1QR, UK

‡e-mail: schweisg@wotan.ens.fr

Cell-fate diversity is generated in part by the unequal segregation of cell-fate determinants during asymmetric cell divisions. In the *Drosophila* pupa, the pI sense organ precursor cell is polarized along the anterior–posterior axis of the fly and divides asymmetrically to generate a posterior pIIa cell and an anterior pIIb cell. The anterior pIIb cell specifically inherits the determinant Numb and the adaptor protein Partner of Numb (Pon). By labelling both the Pon crescent and the microtubules in living pupae, we show that determinants localize at the anterior cortex before mitotic-spindle formation, and that the spindle forms with random orientation and rotates to line up with the Pon crescent. By imaging living *frizzled* (*fz*) mutant pupae we show that Fz regulates the orientation of the polarity axis of pI, the initiation of spindle rotation and the unequal partitioning of determinants. We conclude that Fz participates in establishing the polarity of pI.

The process of unequal segregation of determinants first requires that the mother cell becomes polarized in response to extrinsic or intrinsic signals before mitosis. Cell-fate determinants then localize to one pole of the cell polarity axis and the mitotic spindle lines up with this polarity axis, such that on cytokinesis fate determinants are unequally partitioned to the two daughter cells[1]. An important and largely unresolved issue is how the establishment of cell polarity leads to the asymmetric distribution of cell-fate determinants and to the correct orientation of the mitotic spindle along the cell polarity axis.

In *Drosophila* neuroblasts, which divide asymmetrically along their apical–basal axis, the cell-fate determinant Numb localizes to the basal pole and is specifically segregated into the small basal cell. Basal localization of Numb involves the adaptator protein Partner of Numb (Pon)[2]. An analysis of Pon–GFP (green fluorescent protein) localization in neuroblasts suggested that Pon is first recruited to the cell cortex, then moves along the cortex to form a basal crescent[3]. How the Pon–Numb complex is anchored at the basal pole, once moved there, is not known, but this requires an intact actin cytoskeleton[3,4]. Apical–basal orientation of the spindle results from a 90° rotation during late prophase and metaphase[5]. Both spindle rotation and basal localization of Numb require the activity of *inscuteable* (*insc*)[5,6]. The Insc protein is recruited at the apical cortex by Bazooka (Baz), the fly homologue of Par-3 of *Caenorhabditis elegans* (refs 6–8). How Baz and Insc direct spindle rotation remains unknown, but it has been proposed that one of the two centrosomes may be primed to migrate towards one specific pole of the neuroblast[5]. Centrosome positioning and spindle rotation are thought to involve interactions between astral microtubules and the cell cortex[9]. The dynein–dynactin complex has been suggested to participate in these interactions in the P1 cell of the two-cell stage *C. elegans* embryo[10]. In this cell, the two centrosomes rotate by 90° to line up with a cortical site corresponding to the site of P0 cytokinesis, which is enriched in both dynein and dynactin. In the P1 cell, the two centrosomes appear to be equivalent in their ability to migrate towards this site.

Recent studies have shown that Fz receptors have evolutionarily conserved functions in establishing cell polarity and orientating cell divisions. In *C. elegans*, two receptors of the Fz family, Mom-5 and Lin-17, and their respective Mom-2 and Lin-44 ligands from the Wnt family, have been implicated in polarizing the mother cell before its asymmetric division[11–13]. Regulation of spindle orientation by Mom-5 does not require signalling molecules of the Wnt pathway acting downstream of the GSK-3 kinase, nor does it require gene transcription. Mom-5 activation thus leads to a reorganization of the cell cortex by a pathway distinct from the canonical Wnt pathway[14].

In the *Drosophila* pupa, Fz regulates the asymmetric division of the sensory organ precursor cell, pI. This division takes place within the plane of the epithelium, along the anterior–posterior (A–P) axis of the fly, to generate a posterior pIIa cell and an anterior pIIb cell[15,16]. Numb and Pon accumulate at the anterior pole of pI and specifically segregate into the anterior cell, which therefore adopts the pIIb fate[2,15,17]. In *fz* mutant pupae, the pI cell divides with random orientation relative to the A–P axis, with the crescent of Numb still associated with one randomly positioned spindle pole[15].

By labelling the microtubules in the pI cells of living pupae, we show here that centrosomes do not localize to stereotyped positions before spindle formation and appear to be equivalent. Numb, Pon

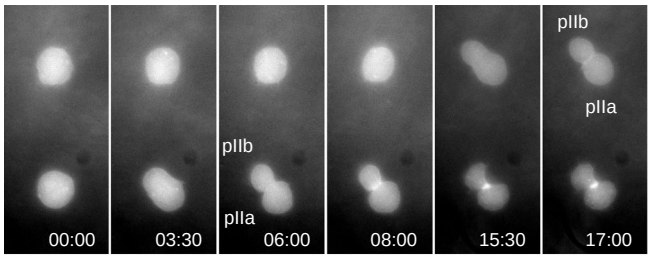

Figure 1 **Time-lapse imaging of the pI division.** Time-lapse imaging of two dividing microchaete pI cells located in row 1. These pI cells, which specifically express gap–GFP under the control of neu^{P72}, divide with a fixed orientation relative to the A–P axis, each generating a small anterior pIIb cell and a large posterior pIIa cell. This difference in size, previously unnoticed, was observed with several GFP markers (gap–GFP, actin–GFP, tau–GFP). In all figures, anterior is up, with the midline on the left.

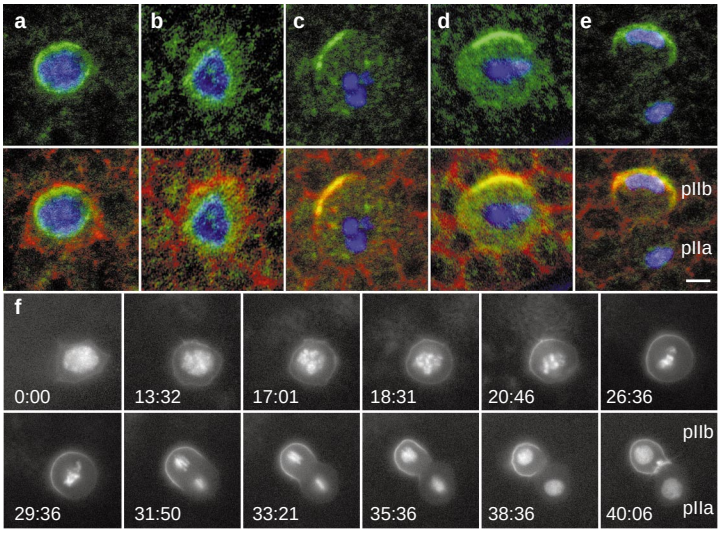

Figure 2 **Pon–GFP accumulates at the anterior cortex during prophase. a–e**, distribution of Numb (red) and Pon (green) in pI cells expressing H2B–YFP (in blue) under the control of neu^{P72} at interphase (**a**), early prophase (**b**), late prophase (**c**), metaphase (**d**) and telophase (**e**). During interphase, Numb localizes to the cortex, whereas Pon accumulates around the nucleus. From late prophase onwards, Numb and Pon colocalize at the anterior cortex. The perinuclear localization of Pon in pI cells contrasts with the apparently uniform cytoplasmic distribution of Pon in neuroblasts at interphase[2]. Scale bar, 5 μm. **f**, Time-lapse imaging of a pI cell expressing both H2B–YFP and Pon–GFP. Progression into mitosis was followed using H2B–YFP to reveal chromatin condensation (t = 13:32), alignment of the chromosomes onto the metaphase plate (t = 29:36), separation and migration of sister chromatids (t = 31:50) and re-formation of daughter nuclei (t = 38:36). Pon–GFP localizes asymmetrically to form an anterior crescent during prophase. Nuclear and perinuclear accumulation of Pon–GFP is masked by H2B–YFP when both markers are expressed (see Fig. 6a).

and Pon–GFP localize to the anterior cortex during prophase, before spindle formation. Alignment of the mitotic spindle with the cell polarity axis involves a rotation of the spindle. Finally, by imaging spindle rotation and localization of Pon–GFP in living *fz* mutant pupae, we show that Fz signalling orientates the axis of polarity and participates in establishing cell polarity itself.

Results

pI divides unequally. Time-lapse imaging of dividing pI cells expressing GFP-tagged proteins was performed in living pupae, using the UAS–GAL4 binary expression system[18]. We generated the neu^{P72} PGAL4 line to express GFP-tagged molecules specifically in pI and its progeny cells (see Methods). In row 1, microchaetae pI cells divide along the A–P axis of the pupa, with a slight tilt toward the midline (Fig. 1, and Supplementary Information movie 1). Time-lapse imaging also reveals that the newly formed pIIb anterior cell is smaller than its pIIa posterior sister (Fig. 1, and Supplementary Information movie 1). We conclude that the division of pI is intrinsically unequal, producing a small anterior pIIb cell and a large pIIa cell.

Pon–GFP accumulates at the anterior pole at late prophase. We first analysed when the cortical crescent containing both Numb and Pon forms at the anterior pole of pI. At interphase, Numb localizes at the cell cortex, with no sign of asymmetric planar distribution, whereas Pon accumulates predominantly around the nucleus (Fig. 2a). Asymmetric localization of Numb at the anterior cortex is first detected at early prophase. At this stage, Pon remains predominantly perinuclear (Fig. 2b). Numb and Pon colocalize at the anterior cortex both at late prophase and during metaphase, and cosegregate into the pIIb cell at telophase (Fig. 2c–e).

A Pon–GFP fusion protein has been shown to be a faithful reporter for Pon asymmetric localization in *Drosophila* neuroblasts[3]. To follow the formation of the Pon crescent, we expressed Pon–GFP specifically in pI cells using neu^{P72}. The time-course distribution of Pon–GFP was analysed in pI cells expressing a Histone2B yellow fluorescent protein (H2B–YFP) that highlights temporal progression into mitosis (Fig. 2f, and Supplementary Information movie 2; see also movie 9). At interphase, Pon–GFP localizes around and within the nucleus, as well as along basal–lateral membranes with no sign of polarized distribution. During prophase, Pon–GFP progressively forms a crescent at the anterior cortex. The position of this crescent does not change from late prophase onward. This crescent is then inherited by the anterior pIIb daughter cell at telophase. We conclude that Pon–GFP localizes asymmetrically at late prophase.

Stereotyped spindle orientation depends on spindle rotation. Unequal segregation of Numb and Pon requires that the mitotic spindle lines up with the Numb–Pon crescent before anaphase. To investigate how and when the mitotic spindle forms and aligns with the cell polarity axis, we examined microtubule distribution in living pupae using GFP fused to the microtubule-binding protein tau[5]. At interphase, microtubules form a dense apical meshwork extending around the nucleus and in long cytoplasmic extensions that retract on mitosis (data not shown). We detected centrosomes by their associated asters about 10 min before spindle formation (Fig. 3a, b, and Supplementary Information movies 3 and 4). They appear in the apical region of pI, at variable positions around the nucleus (Fig. 3c). In 30% of pI cells (n = 20), one centrosome appears to be more closely associated with the nucleus (arrow in Fig. 3a; see ref. 19 for a similar observation in *C. elegans*), and starts migrating around the nucleus before the other centrosome. The initial position of the centrosome relative to the nucleus does not, however, correlate with a specific spindle pole. Indeed, the centrosome found initially closer to the nucleus can later be found at the pIIa pole (n = 3; Fig. 3a) or at the pIIb pole (n = 3).

After separation, the two centrosomes migrate around the nucleus in a largely symmetric manner. Migration is neither restricted to one specific plane nor to one direction. After migration, the axis joining the two centrosomes is randomly orientated. A first rotation movement (αrot1) of the two centrosomes is detected before spindle formation (Fig. 3a, d). The spindle forms

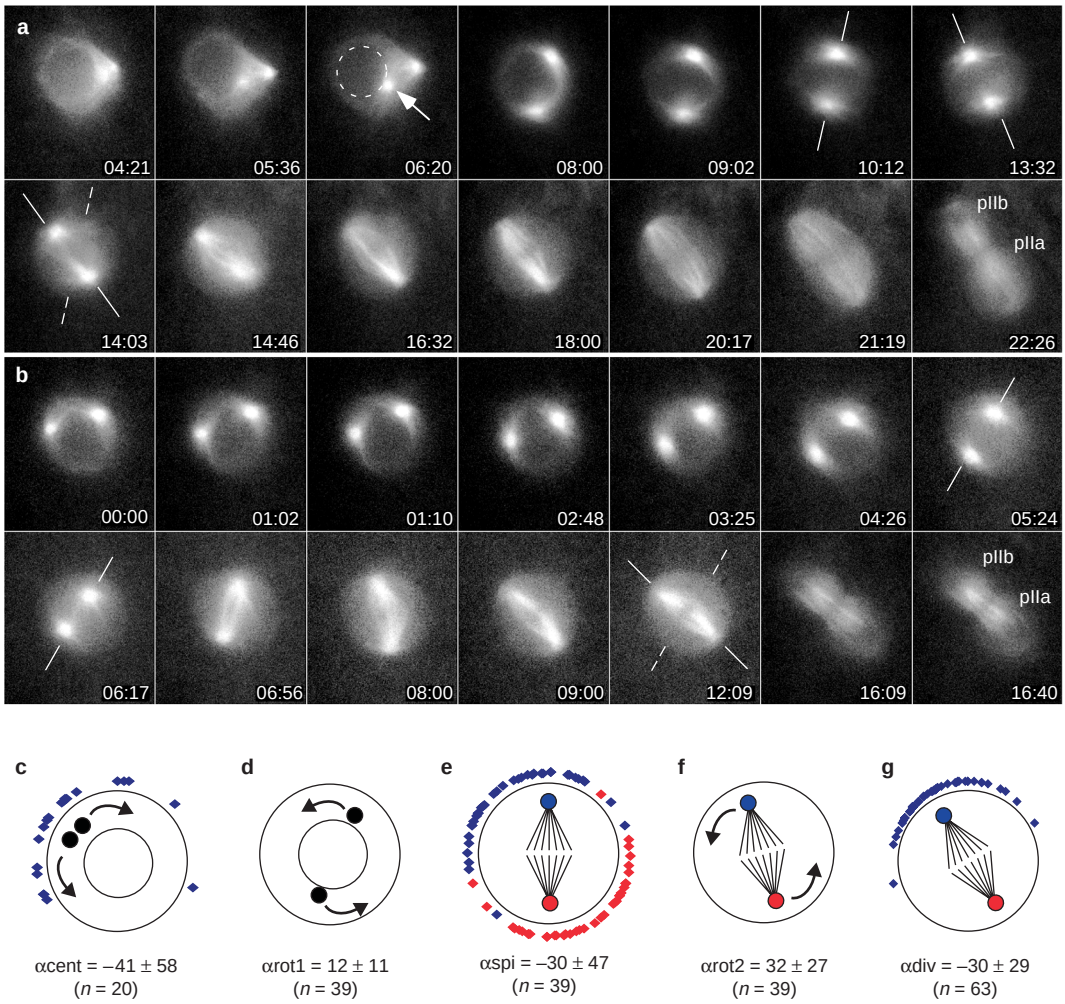

Figure 3 **Centrosome movement and spindle dynamics in pI cells. a**, **b**, Time-lapse imaging of pI cells expressing tau–GFP under the control of neu^{P72}. Centrosome separation (**a**, from t = 4:21 to t = 6:20) and migration (**a**, from t = 6:20 to t = 9:02; **b**, from t = 0:00 to t = 4:26), centrosome and spindle rotation (**a**, from t = 10:12 to t = 16:32; **b**, from t = 5:24 to t = 12:09) and central spindle formation during anaphase-telophase (**a**, from t = 20:17 to 22:26; **b**, from t = 12:09 to t = 16:40) are shown. At t = 6:20, one centrosome (arrow) is localized close to the nucleus (outlined by a dotted line). Rotation movements are highlighted by a line joining the two centrosomes. At t = 14:03 in **a** and t = 12:09 in **b**, the dotted line indicates the position of the two centrosomes at t = 10:12 and t = 5:24, respectively (the angles between these two lines correspond to αrot1 in **a** and αrot2 in **b**). During anaphase and telophase (t = 20:17 and 21:19 in **a**), the spindle becomes progressively asymmetric, correlating with the size difference observed between the two daughter cells (see also ref. 5). **c**–**g**, Centrosome movement and spindle rotation in pI. αcent is the angle between a line joining the cell centre and the duplicated centrosomes and the A–P axis (0° is towards anterior, –90° towards the midline). Centrosomes appear at variable positions in the apical region of pI, with an anterior bias (**c**). Most probably, this bias results from the shape of the pI cells, which often exhibit an anterior apical tilt, both in wild-type and *fz* mutant pupae (see below). Because of this anterior apical tilt, centrosomes that are apical appear to be located anteriorly relative to the more basal nucleus. The values for centrosome rotation observed before (αrot1) and following (αrot2) spindle formation are shown in **d** and **f**. Complete rotation values (αrot1 + αrot2) range from 0 to 105° with a mean value of 44° ± 27. The orientation of the spindle at prometaphase and telophase is shown in **e** and **g**, respectively. Blue and red colours identify the centrosomes eventually inherited by the pIIb and pIIa cells, respectively. αspi (**e**) and αdiv (**g**) correspond to the angles between the A–P axis and the mitotic spindle at prometaphase and telophase, respectively (0° corresponds to a spindle aligned along the A–P axis with the pIIb pole towards the anterior; –90° corresponds to a spindle aligned perpendicular to the A–P axis with the pIIb pole towards the midline).

with no stereotyped orientation (Fig. 3e), and continues to rotate in the same direction (αrot2; Fig. 3f). In 95% of the pI cells (n = 39), the centrosomes rotate by less than 90° in total, and the centrosome located in the anterior region before rotation localizes to the anterior pIIb cell (Fig. 3e, g). We find no correlation between the initial position of centrosomes and the final orientation of the spindle (data not shown). This analysis indicates that spindle orientation is specified after prophase through a regulated rotation of the spindle.

Spindle rotation lines up the mitotic spindle with Pon–GFP. As spindle rotation appears to orientate the spindle relative to the cell's polarity axis, we studied spindle rotation in pI cells expressing both tau–GFP and Pon–GFP. Soon after centrosome migration and roughly 2–3 min before spindle formation, Pon–GFP accumulates at the anterior pole. We find that the orientation of the newly formed spindle does not correlate with the position of the Pon–GFP crescent, and that the spindle rotates, leading to the alignment of the mitotic spindle with asymmetrically distributed Pon–GFP. This results in the unequal segregation of Pon–GFP into the anterior cell (Fig. 4, and Supplementary Information movies 5 and 6). We conclude that Pon–GFP localizes asymmetrically before

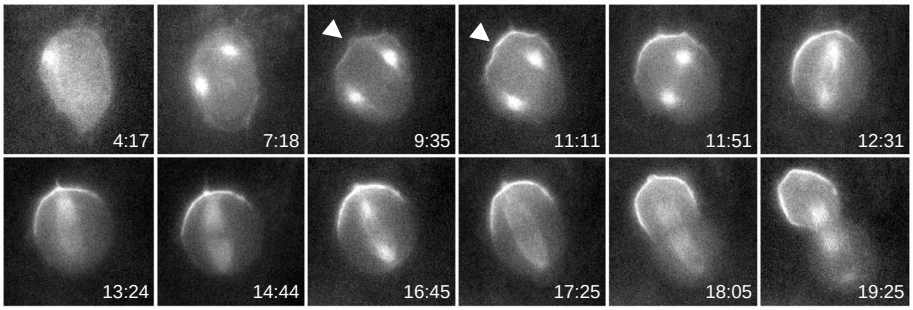

Figure 4 **Spindle rotation directs the unequal segregation of Pon–GFP.** Time-lapse imaging of a pI cell expressing both Pon–GFP and tau–GFP under the control of neu^{P72}, showing formation of the Pon–GFP crescent before spindle formation (arrowheads at t = 9:35 and t = 11:11) and spindle rotation relative to the crescent of Pon–GFP (from t = 11:51 to t = 16:45).

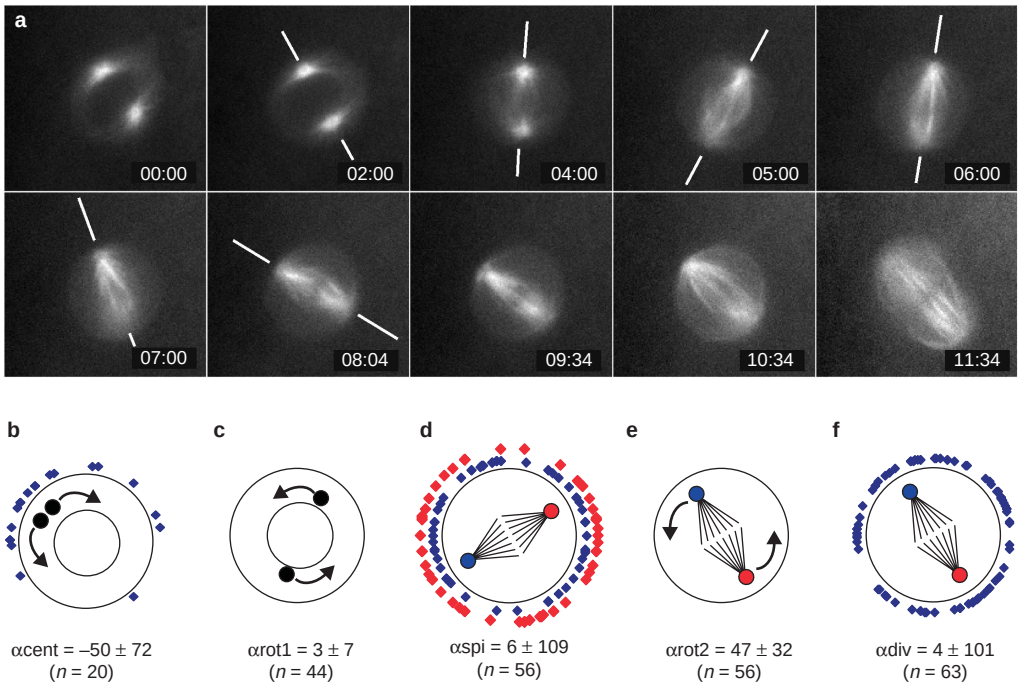

Figure 5 **Centrosome movement and spindle dynamics in *fz* mutant pI cells.** **a**, Time-lapse imaging of a fz^{K21}/fz^{KD4a} mutant pI cell, located in row 1, that expresses tau–GFP under the control of neu^{P72}, showing bidirectional spindle rotation during metaphase (from t = 2:00 to t = 8:34). pI divides with an abnormal orientation relative to the A–P axis, and generates a small cell, identified as pIIb based on its small size. **b–f**, Centrosome and spindle dynamics in fz^{K21}/fz^{KD4a} mutant pI cells. Legend is as in Fig. 2. Centrosomes are intially found at variable positions around the nucleus with an anterior bias (**b**). As mentioned above, this *fz*-independent bias likely results from the shape of the pI cell. At both prometaphase (**d**) and telophase (**f**), mitotic spindles are found randomly orientated. In contrast to wild-type pI cells, *fz* mutant cells show nearly no rotation before spindle formation (**c**): αrot1 in wild-type and *fz* pI cells values are statistically different ($P < 10^{-3}$). Rotation is observed during metaphase (**e**). Complete rotation values (αrot1 + αrot2) are randomly distributed between 0 and 108°, with a mean value of 50 ± 32°.

spindle formation, and that the mitotic spindle is lined up with asymmetrically distributed determinants through spindle rotation.

Fz regulates the initiation of spindle rotation. We previously showed that the orientation of the pI division is regulated by Fz signalling[15]. Here we studied the role of Fz in living mutant pupae expressing tau–GFP (Fig. 5, and Supplementary Information movies 7 and 8). As in wild-type pI cells, centrosomes are initially found at variable positions (Fig. 5b), migrate symmetrically around the nucleus, and the mitotic spindle forms with random orientation relative to the fly body axis (Fig. 5d). In contrast to wild-type pI cells, nearly no centrosome rotation is seen before spindle formation in *fz* mutant pI cells (Fig. 5c, and Supplementary Information movie 8). Rotation greater than 5° is seen in only 12% of *fz* mutant pI cells (n = 44), but rotation greater than 5° is observed in 72% of the wild-type pI cells (n = 39). Rotation initiates after spindle formation, and complete rotation values are similar to those measured in wild-type pI cells (Fig. 5e). In 7% of the mutant pI cells (n = 44), the mitotic spindle rotates in one direction before rotating in the opposite direction (Fig. 5a, and Supplementary Information movie 7). In contrast, bidirectional rotation movements are never observed in wild-type pI cells (n = 39). At anaphase, the spindle is randomly orientated (Fig. 5f; in most cases, the pIIb cell could be

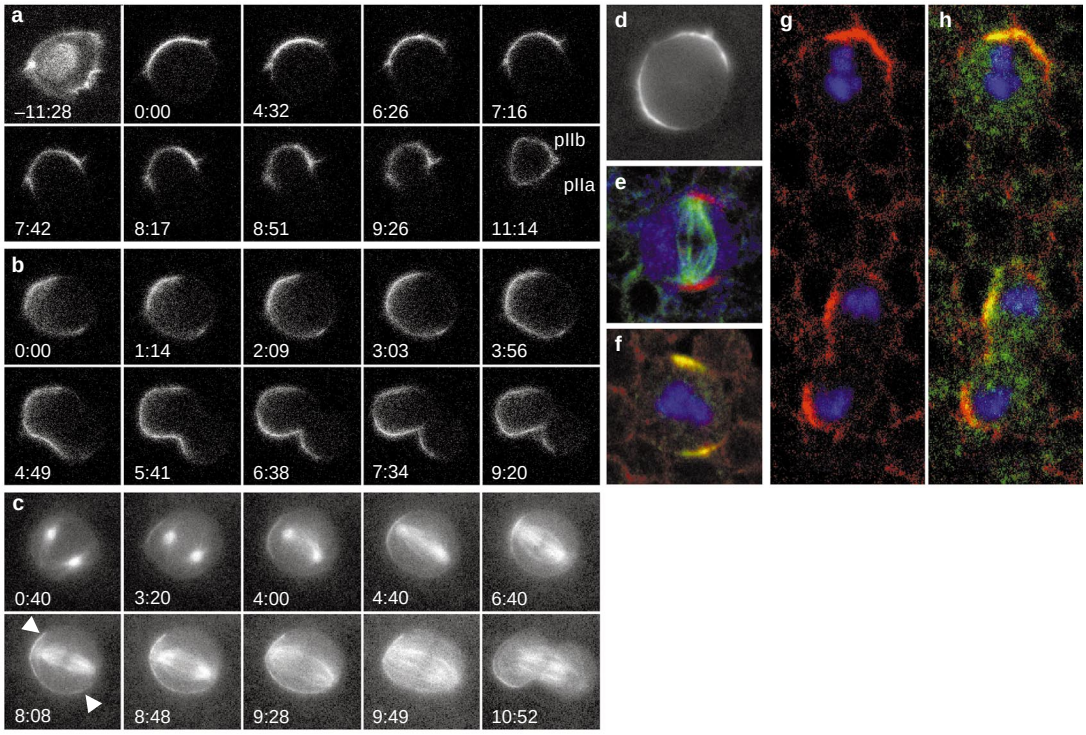

Figure 6 **Defective partitioning of Pon–GFP, Pon and Numb in *fz* mutant pupae. a**, **b**, Time-lapse imaging of control (**a**, *neu*^{P72}*fz*^{KD4a} UAS–Pon–GFP/+) and *fz* mutant (**b**, *fz*^{K21}/*neu*^{P72}*fz*^{KD4a} UAS–Pon–GFP) pI cells expressing Pon–GFP under the control of neu^{P72}. In control pI cells (**a**), Pon–GFP accumulates at the anterior pole during prophase, and segregates into the anterior pIIb cell (n = 28). In *fz* mutant pI cells (**b**), Pon–GFP forms a randomly positioned crescent. In 22% of the *fz* mutant pI cells cytokinesis bisects the Pon–GFP crescent, thereby leading to the segregation of Pon–GFP to both daughter cells. **c**, Time-lapse imaging of a UAS–tau–GFP *fz*^{K21} / *neu*^{P72} *fz*^{KD4a} UAS–Pon–GFP mutant pI cell showing that Pon–GFP starts to form a crescent before spindle formation (arrowhead at t = 3:20), and that the defective segregation of Pon–GFP results from the improper alignment of the mitotic spindle relative to the crescent of Pon–GFP. The extents of the Pon–GFP crescent at the end of metaphase are indicated by arrowheads (at t = 8:08). **d**, Bipolar accumulation of Pon–GFP in a living *fz* mutant pupa. At metaphase, Pon–GFP accumulates at opposite poles and segregates equally into both daughter cells at telophase (not shown). **e**, Bipolar accumulation of Numb (in red) associated with both poles of the mitotic spindle (α-tubulin in green) in a metaphase pI cell (Cut in blue). **f–h**, Immunolocalization of Numb (in red) and Pon (in green) in pI cells expressing H2B–YFP (in blue) under the control of neu^{P72}. Numb and Pon colocalize at one pole (pI cell at the top in **g**, **h,** left and right) or at two opposite poles (**f**) in *fz* mutant pI cells. Bipolar accumulation of Numb leads to the equal segregation of Numb into the two daughter cells (pI cell at the bottom in **g**, **h**, left and right).

identified on the basis of its smaller size). Thus, *fz* is not required for spindle rotation *per se*, yet it appears to regulate when and how rotation occurs. As discussed below, we interpret both the lack of rotation before spindle formation and the bidirectional rotation to suggest that cortical activities involved in centrosome positioning may not be properly polarized in *fz* mutant pI cells.

Fz regulates the unequal segregation of Pon–GFP, Pon and Numb. We next studied the role of Fz in regulating the asymmetric distribution of Pon–GFP. In wild-type pI cells (n = 28), Pon–GFP accumulates at the anterior cortex during prophase and always segregates into the anterior daughter cell (Fig. 6a, and Supplementary Information movie 9). In *fz* mutant pupae, Pon–GFP also accumulates at one cortical pole of pI during prophase, before spindle formation (Fig. 6b, c, and Supplementary Information movies 10–12). This pole, however, is randomly orientated relative to the A–P axis. In 78% of the *fz* mutant pI cells (n = 37), Pon–GFP segregates into only one of the two daughter cells, as in wild-type pI cells. In 22% of the *fz* mutant pI cells, however, Pon–GFP is inherited, at least in part, by both of the two pI daughter cells (Fig. 6b, and Supplementary Information movies 10 and 11). Pon–GFP/tau–GFP double labelling experiments reveal that, in these cells, the mitotic spindle does not properly line up with the Pon–GFP crescent, hence the defective partitioning of Pon–GFP in both daughter cells (Fig. 6c, and Supplementary Information movie 12). Also, the cortical crescent of Pon–GFP appears less restricted in these *fz* mutant pI cells than in wild-type pI cells and may even shift slightly in position around the cell cortex (data not shown). Finally, one cell has a striking bipolar distribution of Pon–GFP (Fig. 6d), eventually leading to the equal segregation of Pon–GFP into both daughter cells (data not shown).

Similar defects could be observed on fixed nota for endogenous Numb in *fz* mutant pI cells. We used the expression of H2B–YFP driven by neu^{P72} to simultaneously identify pI cells and their mitotic stage. In most *fz* mutant pI cells, Numb forms a crescent associated with one spindle pole at metaphase (top cell in Fig. 6g, h) and segregates into one only of the two daughter cells at telophase. These *fz* mutant pI cells are similar to wild-type cells (compare with Fig. 2d, e); however, we also observed *fz* mutant pI cells with a bipolar accumulation of both Numb and Pon at metaphase (Fig. 6e, f), as well as pI cells showing equal segregation of Numb and Pon at telophase (bottom cell in Fig. 6g, h). These observations fully support our time-lapse recordings using Pon–GFP. We conclude that Fz signalling is involved in the formation of a strictly monopolar, anterior crescent containing both Numb and Pon, thereby ensuring the exclusive segregation of Numb at telophase.

Unequal accumulation of Numb in the two pI daughter cells has previously been shown to direct the alternative pIIa/pIIb fate decision[17]. Defective partitioning of Numb is therefore predicted to result in cell-fate transformation. We observed that 5% of *fz*^{K21}/*fz*^{R54} flies have at least one bristle with two shafts and two sockets on the

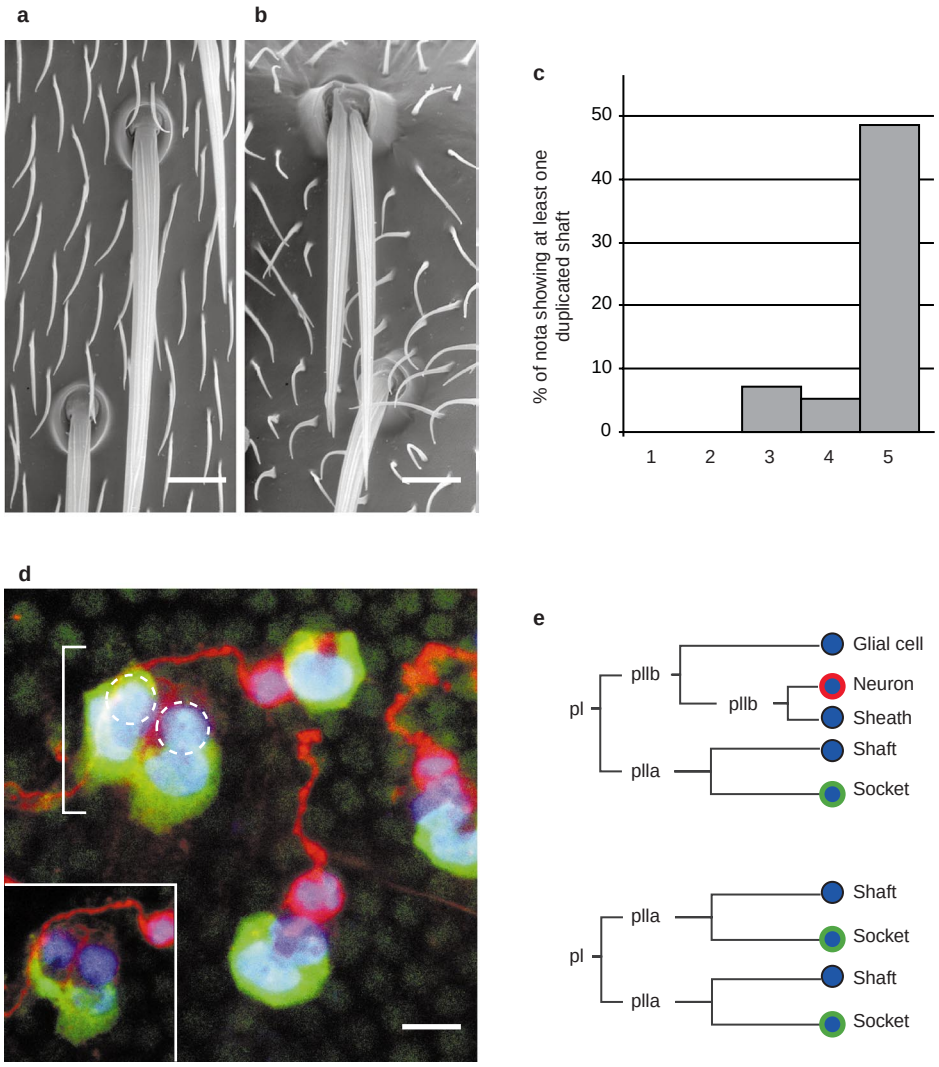

Figure 7 **A *fz-numb* interaction during the pIIa versus pIIb cell-fate decision. a**, **b**, Scanning electron microscopy of a wild-type bristle (**a**) and a double shaft/double socket bristle (**b**) from a $numb^{796}$/+; fz^{K21}/fz^{R54} fly. Scale bar, 10 μm. **c**, Histogram showing the genetic interaction between *fz* and *numb*. No defects are seen in $numb^{796}$/+ (bar 1) and fz^{R54}/TM3 (bar 2) (n = 42). Sense organs with two shafts and two sockets are observed occasionally in $numb^{796}$/+; fz^{K21}/TM3 (bar 3) (7%; n = 42) and in fz^{K21}/fz^{R54} flies (bar 4) (5%; n = 56). By contrast, sense organs with two shafts and two sockets are frequently observed in $numb^{796}$/+; fz^{K21}/fz^{R54} (bar 5) flies (48%; n = 66). **d**, Confocal image showing a sense organ composed of four cells with two socket cells (bracket) and no neuron in a $numb^{+}/numb^{796}$; fz^{K21}/fz^{R54} 24 h after puparium formation (APF) pupa stained for Cut (in blue), Suppressor of Hairless (Su(H), a socket-cell marker, in green) and HRP (a neuron marker, in red). The nuclei of the two Cut-positive, Su(H)-negative cells are outlined by a dotted line. They are subepidermal, as shown in the inset which corresponds to a subepidermal z-section. This suggests that these two cells have acquired a shaft fate. No Prospero-positive sheath cells are found in sense organs containing two Su(H)-positive cells (not shown). Surrounding sense organs have one Su(H)-positive socket cell and one HRP-positive neuron. Scale bar, 10 μm. **e**, Representation of a wild-type lineage[16] and a lineage producing a double shaft-double socket bristle.

notum (see also ref. 20). This bristle phenotype is strongly enhanced by a twofold reduction in *numb* activity (Fig. 7a–c). Sense organs composed of four cells with two socket cells but devoid of either sheath (data not shown) or neuronal cells (Fig. 7d) are observed in the notum of $numb^{796}$/+; fz^{K21}/fz^{R54} pupae. Thus, double socket-double shaft bristles appear to be associated with a loss of pIIb daughter cells, indicating that this phenotype results from a pIIb-to-pIIa transformation (Fig. 7e). These results indicate that *fz* participates in the regulation of the pIIa *vs* pIIb fate decision.

Discussion

We have shown that Numb, Pon and Pon–GFP accumulate at the anterior cortex of pI at late prophase before spindle formation, and that unidirectional rotation of the spindle reorientates the mitotic spindle along the cell polarity axis during prometaphase and metaphase. Centrosome rotation has also been shown to orientate the spindle relative to the cell polarity axis in other asymmetrically dividing cells[5,9,19]. In the two-cell stage *C. elegans* embryo and in the asymmetrically dividing *Drosophila* neuroblast, rotation depends on molecular complexes organized by the Bazooka/Par-3 protein[5–8]. Spindle rotation was also observed in the pIIa and pIIb cells in living *Drosophila* pupae (our own unpublished observations). In pIIb, the spindle rotates from a planar to an apical–basal orientation. The specific accumulation of Insc at the apical pole of pIIb suggests that Insc may regulate this rotation in pIIb as it does in neuroblasts (Y.B. and F.S., unpublished data). The pIIa cell divides in the plane of the epithelium along the A–P axis but in a Fz-independent manner, and

its polarity is regulated by a yet unknown mechanism (R. LeBorgne and F.S., unpublished data). Spindle rotation may be a general mechanism to line up the mitotic spindle with asymmetrically localized cell-fate determinants in cells polarized by Fz-dependent or Fz-independent pathways.

Two models have been proposed to regulate centrosome rotation. In the P1 cell of the two-cell stage *C. elegans* embryo, the two centrosomes are thought to be equivalent and to compete for a cortical mark localized at the anterior pole of the cell, which also corresponds to the point of cytokinesis of P0 (ref. 9). In the *Drosophila* neuroblast, one of the two centrosomes may be primed to rotate in a particular direction[5]. In both cases, however, centrosomes localize to stereotyped positions before rotation. In contrast to both *Drosophila* neuroblasts and the *C. elegans* P1 cell, centrosomes do not occupy stereotyped positions before spindle rotation in pI cells. Centrosomes separate at a variable position within the plane of the epithelium, and migrated symmetrically around the nucleus to occupy random position relative to the A–P axis at prometaphase. Then, each centrosome moves by the shortest path to the closest pole of pI, either anterior or posterior.

These observations suggest that the two centrosomes may be initially equivalent and that centrosomes are captured around prometaphase. Centrosome capture may depend on direct interaction between microtubule-bound proteins and specific cortical proteins. In yeast, the dynein–dynactin complex at the cortex acts redundantly with the proteins Kar9 and Bim1 in directing spindle orientation. Kar9 localizes to defined cortical positions in the bud and directs microtubule orientation towards this site by interacting with the microtubule binding protein Bim1. By analogy, proteins of the EB1/Bim1 family might interact with cortical proteins, such as adenomatous polyposis coli (APC), to direct spindle rotation in multicellular organisms[21,22]. It will thus be of interest to examine whether *Drosophila APC* genes act downstream of *fz* in pI.

Several observations indicate that Fz participates in establishing the polarity of the pI cell, which is revealed by the asymmetric distribution of Numb, Pon and Pon–GFP, as well as by the orientation of the mitotic spindle. First, although spindle rotation occurs in *fz* mutant pI cells, almost no rotation is seen before spindle formation, and rotation is not always strictly unidirectional. Lack of rotation before prometaphase may result from defective localization of the molecules directing spindle rotation. Similarly, bidirectional movement of the spindle indicates that two cortical domains attracting the same centrosome have formed. This suggests that *fz* mutant pI cells may be bipolar. Second, in 22% of the pI cells, the mitotic spindle does not correctly line up with Pon–GFP and cytokinesis bisects the Pon–GFP crescent, leading to the abnormal segregation of Pon–GFP in the pI daughter cells. Finally, bipolar distribution of Numb and Pon at metaphase, and defective segregation of Numb at telophase provide direct evidence for polarity defects. In contrast to these findings, we previously reported that in *fz* mutant pupae pI cells divide with the crescent of Numb tightly associated to one pole of the misorientated spindle[15]. In these experiments, pI was identified as using dA-10 as a marker of sense organ cells. More recently, we found that dA-10 is specifically expressed in pIIa, but not in pI (ref. 16). Here, using neu^{P72} as a pI marker, we have shown in both living and fixed *fz* mutant pupae that pI divides in the plane of the epithelium with a random orientation relative to the A–P axis.

Flamingo (Fmi), like Fz, has been shown to regulate the A–P orientation of the cell polarity axis, but, in contrast to Fz, does not appear to participate in establishing polarity. Indeed, in *fmi* strong hypomorphs, Numb is associated with one pole of the mitotic spindle and segregates into only one of the two daughter cells[23]. Further analysis is required to see whether the difference between the *fz* and *fmi* mutant phenotypes is due to residual *fmi* activity, or instead reflects a functional difference between Fmi and Fz.

The penetrance of the pIIb-to-pIIa transformation phenotype in *fz* mutant flies is much lower than the penetrance of the Pon–GFP segregation defect. This indicates that the pIIa versus pIIb decision takes place normally even when Numb segregates in part to the two daughter cells. We suggest that the well-known feedback loop between the Notch receptor and its two ligands, Delta and Serrate[24] might amplify an initially smaller than usual difference in signalling activity between the two pI daughter cells, therefore rescuing the initial segregation defect of Numb. Also, it may seem surprising at first that both pI daughter cells can adopt a pIIa fate in *fz* mutant pupae, as pIIa does not normally inherit Numb. Indeed, equal segregation of Numb would be predicted to result in the formally opposite cell-fate transformation[2,25]. We suggest that the levels of Numb inherited by the two pI daughter cells in *fz* mutant pupae may be too low to inhibit Notch activation, thus leading to a pIIb-to-pIIa transformation. This interpretation is strongly supported by our observation that the penetrance of this phenotype is enhanced by a decrease in *numb* activity.

In *C. elegans*, *mom-5* mutations fully randomize the orientation of the EMS asymmetric cell division but have only low penetrant effects (5%) on the specification of the EMS daughter cells[12,13]. This suggests that polarity is not fully abolished in *mom-5* mutant embryos. Similarly, in *Drosophila*, Fz-independent mechanisms may be involved in polarizing pI. Indeed, in most *fz* mutant pI cells, Numb, Pon and Pon–GFP localize asymmetrically. At least two models could apply. In the absence of Fz signalling, a cortical site corresponding to the most recent cytokinesis point might serve as a default polarity cue. Such a default pathway operates in the budding yeast to determine the localization of Cdc24 at the cortex in the absence of signalling by pheromone receptors[26]. Alternatively, the formation of a specialized region at the cell cortex might involve positive feedback loop and auto-assembly mechanisms, such that small differences in the activity of the signalling molecules directing crescent formation could be converted into a monopolar asymmetry.

In *fz* mutant pI cells, these mechanisms would promote the formation of a randomly positioned crescent from uniformly distributed components (and sometimes two, when two equivalent 'nucleation' points form at opposite poles). Notably, in *Drosophila* neuroblasts, the existence of a second *baz*/*insc*-independent mechanism has been suggested to account for the mostly normal segregation of fate determinants at telophase observed in *insc* and *baz* mutant embryos[8]. It is possible that these auto-assembly and positive feedback loops mechanisms also account for this *baz*/*insc*-independent mechanism. Fz signalling, and possibly Insc, may regulate these auto-assembly and/or positive feedback loop activities by providing a spatial input, thus ensuring that the asymmetric distribution of fate determinants is efficiently coordinated with spindle orientation. □

Methods

Flies.

The neu^{P72} PGAL4 insertion line was obtained by P-element conversion of the PlacZ A101 allele of *neuralised*^{P7}. An X-linked PGAL4 was mobilized using the P-element transposase in the germ-line of males carrying A101 as a recipient P element in a transposase-mediated P-element conversion: 180 *w* PGAL4 / Y ; *neuP*[*ry*$^{+}$] *A101 H*^{C28} / TM3 Sb Δ2-3 males were individually crossed to *w*^{1118} females, and 76 independent jumps on the third chromosome were selected. From these 76 PGAL4 lines, 30 expressed UAS–GFP in pI. One line, neu^{P72}, was selected and used here.

DNA encoding human histone H2B was isolated as a 378-base-pair *Kpn*I–*Bam*HI fragment from H2BGFP-N1 (ref. 28). The mYFP yellow-shifted GFP variant[29] was amplified by polymerase chain reaction as a *Bam*HI–*Xba*I fragment. These fragments were subcloned by three way ligation into *Kpn*I–*Xba*I-digested pUAST (ref. 18) to give UAS–H2B–mYFP. Transgenic lines were generated by DNA injection into yw; Δ2-3Sb/TM6 embryos.

Other GFP markers were UAS–Pon–GFP (a kind gift from Y.-N. Jan)[3], UAS–tau–GFP[5], UAS–actin–GFP (kindly provide by A. Martinez-Arias)[30], and UAS–gap–GFP (a membrane-associated enhanced GFP kindly provided by E. Spana). Expression of tau–GFP using neu^{P72} had no effect on mitosis duration and spindle orientation in pI, when compared with nls–GFP or H2B (data not shown). Furthermore, the divisions of pIIb, pIIa and pIIIb in neu^{P72} tau–GFP pupae were correctly orientated, no cell-fate changes were detected, and no bristle differentiation defects were observed in neu^{P72} tau–GFP adults following imaging. Thus, expression of tau–GFP in neu^{P72} tau–GFP pupae had no detectable effect in this lineage.

Kd4a and K21 are null alleles of *fz*, whereas R54 is a strong loss-of-function allele[15]. The allele 796 of *numb* is one of the strongest known allele of *numb*.

GFP imaging.

GFP imaging was performed on non-Tb pupae from the following crosses: (1) UAS–gap–GFP × neu^{P72} / TM6b, Tb; (2) UAS–H2B–GFP ; neu^{P72} UAS–Pon–GFP / TM6b Tb × UAS–Pon–GFP; (3) UAS–tau–GFP / TM6b, Tb × neu^{P72} / TM6b, Tb; (4) UAS–tau–GFP fz^{K21} / TM6b, Tb × neu^{P72} fz^{Kd4a}/ TM6b, Tb; (5) neu^{P72} UAS–tau–GFP / TM6b, Tb × UAS–Pon–GFP; (6) fz^{K21} / TM6b, Tb × neu^{P72} fz^{Kd4a} UAS–Pon–GFP / TM6b, Tb; (7) UAS–tau–GFP fz^{K21} / TM6b, Tb × neu^{P72} fz^{Kd4a} UAS–Pon–GFP / TM6b, Tb; (8) y w × neu^{P72} fzKD4a UAS–Pon–GFP / TM6b, Tb.

Living pupae were adhered to double-sided tape in between stacks of 4–5 coverslips, with the notum facing up. The pupal case covering the head and notum was removed, and a coverslip, coated with Voltalef 10S oil on its bottom surface, was gently apposed onto pupae. Microchaete pI cells were imaged either on a Leica TCS 4D confocal microscope (×63 oil immersion objective), or on Leica DML and DMRXA microscopes (×40 or ×63 immersion oil objective) equipped with a Princeton Instruments Micromax Camera (exposure time was 200 ms and images were acquired every 20–60 s) driven by Metamorph software (Universal Imaging). Time-lapse movies were assembled using Metamorph and NIH image software.

Immunocytochemistry.

Dissected nota were processed as previously described[31]. Primary antibodies were rabbit anti-Pon (a gift from Y. N. Jan; 1:1000), guinea-pig anti-Numb (a gift from Y. N. Jan; 1:1000), rat anti-α-tubulin (Serotec; 1:3,000), rabbit anti-horseradish peroxidase (HRP) (1:1,000; a gift from J.-R. Martin), rat anti-Su(H) (1:1,000), mouse anti-Cut (2B10, DSHB; 1:500). All Alexa-coupled secondary antibodies were from Molecular Probes.

RECEIVED 7 JULY; REVISED 6 SEPTEMBER; ACCEPTED 4 OCTOBER 1999;
PUBLISHED 6 DECEMBER 2000

1. Jan, Y. N. & Jan, L. Y. Polarity in cell division: what frames thy fearful asymmetry? *Cell* **100,** 599–602 (2000).
2. Lu, B., Rothenberg, M., Jan, L. Y. & Jan, Y. N. Partner of Numb colocalizes with Numb during mitosis and directs Numb asymmetric localization in *Drosophila* neural and muscle progenitors. *Cell* **95,** 225–235 (1998).
3. Lu, B., Ackerman, L., Jan, L. Y. & Jan, Y.-N. Modes of protein movement that lead to the asymmetric localization of Partner of Numb during *Drosophila* neuroblast division. *Mol. Cell* **4,** 883–891 (1999).
4. Knoblich, J. A., Jan, L. Y. & Jan, Y. N. The N terminus of the *Drosophila* Numb protein directs membrane association and actin-dependent asymmetric localization. *Proc. Natl Acad. Sci. USA* **94,** 13005–13010 (1997).
5. Kaltschmidt, J. A., Davidson, C. M., Brown, N. H. & Brand, A. H. Rotation and asymmetry of the mitotic spindle direct asymmetric cell division in the developing central nervous system *Nature Cell Biol.* **2,** 7–12 (2000).
6. Kraut, R., Chia, W., Jan, L. Y., Jan, Y. N. & Knoblich, J. A. Role of inscuteable in orienting asymmetric cell divisions in *Drosophila. Nature* **383,** 50–55 (1996).
7. Wodarz, A., Ramrath, A., Kuchinke, U. & Knust, E. Bazooka provides an apical cue for Inscuteable localization in *Drosophila* neuroblasts. *Nature* **402,** 544–547 (1999).
8. Schober, M., Schaefer, M. & Knoblich, J. A. Bazooka recruits Inscuteable to orient asymmetric cell divisions in *Drosophila* neuroblasts. *Nature* **402,** 548–551 (1999).
9. Hyman, A. A. Centrosome movement in the early divisions of Caenorhabditis elegans: a cortical site determining centrosome position. *J. Cell Biol.* **109,** 1185–1193 (1989).
10. Skop, A. R. & White, J. G. The dynactin complex is required for cleavage plane specification in early Caenorhabditis elegans embryos. *Curr. Biol.* **8,** 1110–1116 (1998).
11. Sawa, H., Lobel, L. & Horvitz, H. R. The Caenorhabditis elegans gene lin-17, which is required for certain asymmetric cell divisions, encodes a putative seven-transmembrane protein similar to the *Drosophila* frizzled protein. *Genes Dev.* **10,** 2189–2197 (1996).
12. Thorpe, C. J., Schlesinger, A., Carter, J. C. & Bowerman, B. Wnt signaling polarizes an early *C. elegans* blastomere to distinguish endoderm from mesoderm *Cell* **90,** 695–705 (1997).
13. Rocheleau, C. E. *et al.* Wnt signaling and an APC-related gene specify endoderm in early *C. elegans* embryos. *Cell* **90,** 707–716 (1997).
14. Schlesinger, A., Shelton, C. A., Maloof, J. N., Meneghini, M. & Bowerman, B. Wnt pathway components orient a mitotic spindle in the early Caenorhabditis elegans embryo without requiring gene transcription in the responding cell. *Genes Dev.* **13,** 2028–2038 (1999).
15. Gho, M. & Schweisguth, F. Frizzled signalling controls orientation of asymmetric sense organ precursor cell divisions in *Drosophila. Nature* **393,** 178–181 (1998).
16. Gho, M., Bellaiche, Y. & Schweisguth, F. Revisiting the *Drosophila* microchaete lineage: a novel intrinsically asymmetric cell division generates a glial cell. *Development* **126,** 3573–3584 (1999).
17. Rhyu, M. S., Jan, L. Y. & Jan, Y. N. Asymmetric distribution of numb protein during division of the sensory organ precursor cell confers distinct fates to daughter cells *Cell* **76,** 477–491 (1994).
18. Brand, A. H. & Perrimon, N. Targeted gene expression as a means of altering cell fates and generating dominant phenotypes. *Development* **118,** 401–415 (1993).
19. Keating, H. H. & White, J. G. Centrosome dynamics in early embryos of Caenorhabditis elegans. *J. Cell Sci.* **111,** 3027–3033 (1998).
20. Adler, P. N., Charlton, J. & Vinson, C. Allelic variations at the frizzled locus of *Drosophila. Dev. Genet.* **8,** 99–119 (1987).
21. Lee, L. *et al.* Positioning of the mitotic spindle by a cortical-microtubule capture mechanism. *Science* **287,** 2260–2262 (2000).
22. Korinek, W. S., Copeland, M. J., Chaudhuri, A. & Chant, J. Molecular linkage underlying microtubule orientation toward cortical sites in yeast. *Science* **287,** 2257–2259 (2000).
23. Lu, B., Usui, T., Uemura, T., Jan, L. & Jan, Y. N. Flamingo controls the planar polarity of sensory bristles and asymmetric division of sensory organ precursors in *Drosophila. Curr. Biol.* **9,** 1247–1250 (1999).
24. Heitzler, P. & Simpson, P. The choice of cell fate in the epidermis of *Drosophila. Cell* **64,** 1083–1092 (1991).
25. Buescher, M. *et al.* Binary sibling neuronal cell fate decisions in the *Drosophila* embryonic central nervous system are nonstochastic and require inscuteable-mediated asymmetry of ganglion mother cells. *Genes Dev.* **12,** 1858–1870 (1998).
26. Nern, A. & Arkowitz, R. A. A Cdc24p-Far1p-Gbetagamma protein complex required for yeast orientation during mating. *J. Cell Biol.* **144,** 1187–1202 (1999).
27. Usui, K. & Kimura, K.-i. Sequential emergence of the evenly spaced microchaetes on the notum of *Drosophila. Roux's Arch. Dev. Biol.* **203,** 151–158 (1993).
28. Kanda, T., Sullivan, K. F. & Wahl, G. M. Histone–GFP fusion protein enables sensitive analysis of chromosome dynamics in living mammalian cells. *Curr. Biol.* **8,** 377–385 (1998).
29. Haseloff, J., Dormand, E.-L. & Brand, A. H. in *Protocols in Confocal Microscopy* (Humana Press, 1999).
30. Verkhusha, V. V., Tsukita, S. & Oda, H. Actin dynamics in lamellipodia of migrating border cells in the *Drosophila* ovary revealed by a GFP–actin fusion protein. *FEBS Lett.* **445,** 395–401 (1999).
31. Gho, M., Lecourtois, M., Geraud, G., Posakony, J. W. & Schweisguth, F. Subcellular localization of Suppressor of Hairless in *Drosophila* sense organ cells during Notch signalling. *Development* **122,** 1673–1682 (1996).

ACKNOWLEDGEMENTS

We thank P. Adler, W. Chia, Y.-N. Jan, T. Kanda, B.-W. Lu, N. Perrimon, J.-R. Martin, A. Martinez-Arias, E. Spana, G. M. Wahl and the Developmental Studies Hybridoma Bank for antibodies, plasmids and flies. We also thank G. Géraud and the confocal imaging facility of the Institut Jacques Monod, as well as the Electron Microscopy Facility of the University Paris 6 for use of confocal and SEM microscopes. We thank A. Martinez-Arias, P. van Roessel and R. LeBorgne for critical reading. This work was supported in part by grants from the Centre National de la Recherche Scientifique (ATIPE), the Association pour la Recherche contre le Cancer (ARC 5951) and by the Wellcome Trust.
Correspondence and requests for materials should be addressed to F.S. Supplementary information is available on *Nature Cell Biology*'s website (http://cellbio.nature.com) or as paper copy from the London editorial office of *Nature Cell Biology*.

Movie 1: pI divides unequally with a stereotyped planar orientation

Wide-field time-lapse imaging of two dividing microchaete pI cells located in row 1. These pI cells, which specifically express gap-GFP under the control of neu^{P72}, divide with a fixed orientation relative to the a-p axis, each generating a small anterior pIIb cell and a large posterior cell. Anterior is up.

Movie 2: Pon-GFP accumulates at the anterior cortex during prophase

Wide-field time-lapse imaging of a pI cell expressing both Histone2B-YFP and Pon-GFP. Progression into mitosis was followed using H2B-YFP to reveal chromatin condensation, alignment of the chromosomes onto the metaphase plate, chromosome migration to the pole and re-formation of daughter nuclei. Pon-GFP localises to the anterior cortex at late prophase. The perinuclear accumulation of Pon-GFP is masked by H2B-YFP. Anterior is up.

Movie 3: Centrosome movement and spindle dynamics in pI cells (1)

Wide-field time-lapse imaging of pI cells expressing tau-GFP under the control of neu^{P72}, showing centrosome separation and migration, mitotic spindle formation at prometaphase followed by a 45° rotation. In this movie, the centrosome that is eventually inherited by the posterior pIIb cell is closely associated with the nucleus and starts migrating around the nucleus before the other centrosome. The initial position of the centrosome relative to the nucleus does not, however, correlate with a specific spindle pole. Also, centrosome rotation starts prior to spindle formation. Anterior is up.

Movie 4: Centrosome movement and spindle dynamics in pI cells (2)

Wide-field time-lapse imaging of pI cells expressing tau-GFP under the control of neu^{P72}, showing a nearly 90° spindle rotation. Anterior is up.

Movie 5: Spindle rotation directs the unequal segregation of Pon-GFP (1)

Wide-field time-lapse imaging of a pI cell expressing both Pon-GFP and tau-GFP under the control of neu^{P72}, showing formation of the Pon-GFP crescent prior to spindle formation and spindle rotation relative to the crescent of Pon-GFP. Anterior is up.

Movie 6: Spindle rotation directs the unequal segregation of Pon-GFP (2)

Wide-field time-lapse imaging of a pI cell expressing both Pon-GFP and tau-GFP under the control of neu^{P72}, showing that the spindle rotates by 90° to line up with the anterior crescent of Pon-GFP. Anterior is up.

Movie 7: Spindle rotation and orientation in *frizzled* mutant pI cells (1)

Wide-field time-lapse imaging of a fz^{K21}/fz^{KD4a} mutant pI cell that expresses tau-GFP under the control of neu^{P72}, showing bidirectional spindle rotation during metaphase. pI divides with an abnormal orientation relative to the a-p axis, and generates a small pIIb cell toward the posterior pole (bottom-right corner). Anterior is up.

Movie 8: Spindle rotation and orientation in *frizzled* mutant pI cells (2)

Confocal time-lapse imaging of a fz^{K21}/fz^{KD4a} mutant pI cell that expresses tau-GFP under the control of neu^{P72}. Anterior is up.

Movie 9: Pon-GFP accumulates at the anterior cortex during prophase

Confocal time-lapse imaging of a control neu^{P72} fz^{KD4a} UAS-Pon-GFP / + pI cell expressing Pon-GFP under the control of neu^{P72}. Pon-GFP is intially found around the nucleus and in basal cytoplasmic extensions that retract during prophase. Pon-GFP accumulates at the anterior pole during prophase, and segregates into the anterior pIIb cell. Anterior is up.

Movie 10: Unequal segregation of Pon-GFP in *frizzled* mutant pI cells (1)

Confocal time-lapse imaging of a fz^{K21} / neu^{P72} fz^{KD4a} UAS-Pon-GFP mutant pI cells. Pon-GFP forms a randomly positioned crescent in *fz* mutant pI cells. In this movie, Pon-GFP localises in an abnormally large lateral crescent, and cytokinesis bisects this Pon-GFP crescent, thereby leading to the segregation of Pon-GFP to both daughter cells. Anterior is up.

Movie 11: Unequal segregation of Pon-GFP in *frizzled* mutant pI cells (2)

Wide-field time-lapse imaging of a fz^{K21} / neu^{P72} fz^{KD4a} UAS-Pon-GFP mutant pI cells. Pon-GFP forms a randomly positioned crescent in *fz* mutant pI cells. In this movie, Pon-GFP localises in an abnormally large posterior crescent and cytokinesis bisects this Pon-GFP crescent, thereby leading to the segregation of Pon-GFP to both daughter cells. Anterior is up.

Movie 12: Unequal segregation of Pon-GFP in *frizzled* mutant pI cells (3)

Wide-field time-lapse imaging of a fz^{K21} UAS-tau-GFP / neu^{P72} fz^{KD4a} UAS-Pon-GFP mutant pI cells. Pon-GFP localises asymmetrically prior to spindle formation and forms a large posterior crescent. In this pI cell, the spindle does not rotate significantly, and does not line up with the center of the Pon-GFP crescent, thereby leading to the partial mis-partitionning of Pon-GFP to both daughter cells. Anterior is up.